TẠP CHÍ KHOA HỌC VÀ CÔNG NGHỆ ĐẠI HỌC DUY TÂN
DTU Journal of Science and Technology 05(78) (226) 19-27

ĐẠI HỌC DUY TÂN
DUYTAN UNIVERSITY

Evaluation of the Antibacterial and Anti-Biofilm Potential of Silver Nanoparticles Synthesized Using Basil (*Ocimum basilicum* L.) Leaf Extract

Đánh giá tiềm năng kháng khuẩn và kháng màng sinh học của hệ nano bạc được tổng hợp từ dịch chiết lá Húng quế (*Ocimum basilicum* L.)

Cao Tuyet Nghi[a], Nguyen Thi Bich Tram[a], Nguyen Tran Truc Phuong[b, c], Trinh Thi Ngoc Diep[d*]
Cao Tuyết Nghi[a], Nguyễn Thị Bích Trâm[a], Nguyễn Trần Trúc Phương[b, c], Trịnh Thị Ngọc Diệp[d*]

[a]*School of Agriculture and Aquaculture, Tra Vinh University, Vinh Long, Vietnam*
[a]*Khoa Nông nghiệp – Thủy sản, Đại học Trà Vinh, Vĩnh Long, Việt Nam*
[b]*NTT Hi-Tech Institute, Nguyen Tat Thanh University, Ho Chi Minh City, 70000, Vietnam*
[b]*Viện Kỹ thuật Công nghệ cao NTT, Trường Đại học Nguyễn Tất Thành, Thành phố Hồ Chí Minh, 70000, Việt Nam*
[c]*Nguyen Tat Thanh University Center for Hi-Tech Development, Saigon Hi-Tech Park, Ho Chi Minh City, 70000, Vietnam*
[c]*Trung tâm Phát triển Công nghệ cao, Trường Đại học Nguyễn Tất Thành, Khu Công nghệ cao Sài Gòn, Thành phố Hồ Chí Minh, 70000, Việt Nam*
[d]*Biotechnology Institute, Tra Vinh University, Vinh Long, Vietnam*
[d]*Viện Công nghệ Sinh học, Đại học Trà Vinh, Vĩnh Long, Việt Nam*

(Date of receiving article: 26/06/2026, date of completion of review: 23/07/2026, date of acceptance for posting: 12/09/2026)

Abstract

This study aimed to evaluate the antibacterial and anti-biofilm potential of silver nanoparticles (AgNPs) synthesized using *Ocimum basilicum* L. leaf extract. The synthesized nanomaterial was characterized by UV-Vis spectroscopy, X-ray diffraction (XRD), and scanning electron microscopy (SEM). These results showed that AgNPs had a high-homogeneity of size distribution of 39.19 ± 2.7 nm, and a single UV-Vis absorbance band was obtained at ~410 nm. These results confirmed the successful synthesis of AgNPs. Antibacterial activity of the materials was assessed using the agar diffusion method, demonstrating a concentration-dependent inhibitory effect against *Enterococcus faecalis* with the inhibition zone of 4.33 mm in diameter at the concentration of 0.646 nM. The anti-biofilm activity was determined by a crystal violet staining assay, which revealed a significant reduction in biofilm formation (approximately 50%) in AgNPs-treated samples compared to the control group. Overall, the findings indicated that biologically synthesized AgNPs effectively inhibited both planktonic bacterial cells and biofilm formation. This study provides further insight into the development of environmentally friendly nanomaterials with promising applications in infection control strategies.

Keywords: antibacterial activity, anti-biofilm activity, green synthesis, silver nanoparticles (AgNPs), *Enterococcus faecalis*, *Ocimum basilicum*

Tóm tắt

Nghiên cứu này nhằm đánh giá tiềm năng kháng khuẩn và kháng màng sinh học của các hạt nano bạc (AgNPs) được tổng hợp bằng dịch chiết lá *Ocimum basilicum* L. Vật liệu nano tổng hợp được phân tích bằng quang phổ UV-Vis, nhiễu xạ tia X (XRD) và kính hiển vi điện tử quét (SEM). Kết quả cho thấy AgNPs có kích thước trung bình 39,19 ± 2,7 nm

[*]*Tác giả liên hệ*: Trịnh Thị Ngọc Diệp
Email: ttndiep@tvu.edu.vn

với phân bố kích thước đồng đều, và có đỉnh hấp thụ UV-Vis tại khoảng 410 nm. Những kết quả này xác nhận sự tổng hợp thành công AgNPs. Hoạt tính kháng khuẩn của vật liệu được đánh giá bằng phương pháp khuếch tán trên thạch, cho thấy tác dụng ức chế phụ thuộc vào nồng độ đối với *Enterococcus faecalis* với vùng ức chế có đường kính 4,33 mm ở nồng độ 0,646 nM. Hoạt tính kháng màng sinh học được xác định bằng phương pháp nhuộm với tím tinh thể, cho thấy giảm đáng kể sự hình thành màng sinh học (khoảng 50%) ở các mẫu được xử lý bằng AgNPs so với nhóm đối chứng. Nhìn chung, các phát hiện cho thấy AgNPs được tổng hợp sinh học có hiệu quả trong việc ức chế cả tế bào vi khuẩn đơn lẻ và sự hình thành màng sinh học. Nghiên cứu này cung cấp thêm hiểu biết về sự phát triển của các vật liệu nano thân thiện với môi trường, có tiềm năng ứng dụng trong các chiến lược kiểm soát nhiễm trùng.

Từ khóa: hoạt tính kháng khuẩn, hoạt tính kháng màng sinh học, tổng hợp xanh, hạt nano bạc (AgNPs), *Enterococcus faecalis*, *Ocimum basilicum*

1. Introduction

In recent years, the increasing prevalence of antibiotic-resistant bacterial strains has become a global concern, particularly in public healthcare. Pathogenic bacteria such as *Enterococcus faecalis (E. faecalis), Escherichia coli (E. coli), Pseudomonas aeruginosa (P. aeruginosa), Staphylococcus aureus (S. aureus), Klebsiella pneumoniae (K. pneumoniae)*, and *Acinetobacter baumannii (A. baumannii)* can form biofilms on medical devices and living tissues, resulting in chronic, recurrent, and severe infections. It is estimated that approximately 80% of chronic human infections are associated with biofilm formation (Costerton et al. [1]).

AgNPs exhibit broad-spectrum antibacterial and anti-biofilm activities through multiple mechanisms, including disruption of the extracellular polymeric matrix and interference with quorum sensing, ultimately inhibiting bacterial growth and biofilm development [2, 3]. Green synthesis using plant extracts has emerged as an eco-friendly and sustainable approach for AgNPs production. Previous studies have successfully synthesized AgNPs using *Aloe vera*, garlic, green tea, papaya, and other plant extracts, demonstrating promising possibility for green synthesis of nanoparticles [4, 5, 6, 7, 8].

Ocimum basilicum L. (basil) is a medicinal plant rich in bioactive compounds with reported antibacterial and antioxidant activities [9, 10, 11]. However, studies on basil-mediated AgNPs, particularly their anti-biofilm potential, remain limited. Therefore, this study aimed to synthesize AgNPs using basil leaf extract via a green synthesis approach, characterize the nanoparticles by UV-Vis spectroscopy, X-ray diffraction (XRD), and scanning electron microscopy (SEM), and evaluate their antibacterial and anti-biofilm activities.

2. Materials and methods

2.1. Materials

Fresh basil leaves were collected from Vinh Long province. Silver nitrate ($AgNO_3$, 99%) was purchased from Sigma-Aldrich. Mueller Hinton Agar (MHA) and Luria Bertani Broth (LB) were purchased from Himedia. Crystal violet was from Phu Sa. Ethanol and methanol were from Xilong.

2.2. Methods

2.2.1. Synthesis of AgNPs

Basil leaves were carefully selected to remove old and damaged parts. The fresh ones were washed with sterile water and dried until constant weight. The dried leaf samples were stored at room temperature and used for further experiments. Water was employed to extract the sample at a ratio of 1/10 (w/v). The sample was then heated at 90 °C for 30 min to receive the aqueous extract. The mixture was prepared by combining the 10 mM $AgNO_3$ solution with the aqueous extract at different concentrations, as in Table 1.

Table 1. Treatments using different concentrations of silver nitrate

Treatment	Silver nitrate (10 mM) (mL)	Aqueous extract (mL)	Water (mL)	Final volume (mL)
1	1	1	3	5
2	2	1	2	5
3	3	1	1	5
4	4	1	0	5

The mixture was then stirred at 500 rpm at room temperature for 30 min until the color was unchanged. The materials were stored at 4°C for further experiments.

2.2.2. Characterization of synthesized materials

The optical properties of AgNPs solutions were recorded by the Cary 60 UV-Vis spectrophotometer with a rate of 4800 nm/min in the range of 300-1000 nm. The Bruker D8 Advance Powder X-ray diffractometer was used to determine the crystal structure of AgNPs over the range of 30-80°. Field emission scanning electron microscope (Hitachi Regulus 8100 SEM, Japan) was used to observe the shape and size of AgNPs at a voltage of 5 kV. Dynamic light scattering (DLS) spectroscopy was used to assess the size distribution of AgNPs in solution.

2.2.3. Evaluation of the antibacterial activity of AgNPs

The antibacterial activity of AgNPs was evaluated using the agar well diffusion method on Mueller-Hinton agar (MHA).

The bacterial suspension of *E. faecalis* was adjusted to a turbidity equivalent to 0.5 McFarland standard, after which the suspension was dropped onto MHA plates and evenly spread over the agar surface using a sterile triangular spreader. On each agar plate, five wells of uniform diameter were aseptically punched. One well without any sample was used as the negative control, while the remaining three wells were each loaded with 100 µL of the test solution.

AgNPs solutions synthesized under four different experimental conditions from the previous experiment were used to assess antibacterial activity. After the sample application, the agar plates were incubated at 35-37°C for 24-48 hours. The antibacterial effect was determined based on the presence and diameter of inhibition zones formed around the wells. Diameters of inhibition zones of different experimental conditions were collected and analysed. Each treatment was repeated three times. In addition, $AgNO_3$ at the concentration of 10 mM and aqueous basil extract were used as controls.

2.2.4. Evaluation of the anti-biofilm activity of AgNPs

The anti-biofilm activity of AgNPs was investigated using the crystal violet staining method. *E. faecalis* was cultured overnight in sterile Eppendorf tubes to allow biofilm formation on the inner surface of the tubes. To evaluate the anti-biofilm potential of the material, the AgNPs solution exhibiting the strongest antibacterial activity in the previous experiment was selected. The AgNPs solution was added to the tubes containing *E. faecalis* and the culture medium.

For comparison, tubes containing bacteria and medium alone and tubes containing bacteria, medium, and antibiotic were used as the test sample, positive and negative controls, respectively. After incubation, the culture supernatant was gently removed, and the remaining biofilm was subjected to further treatment.

Following treatment, the biofilm was gently washed with sterile distilled water to remove non-adherent cells and subsequently stained with crystal violet. After the destaining process to remove unbound dye, absorbance was measured at 570 nm. The obtained results were used to evaluate the anti-biofilm efficacy of AgNPs in comparison with the control samples.

3. Results and discussion

3.1. Optical properties and crystalline structure of AgNPs

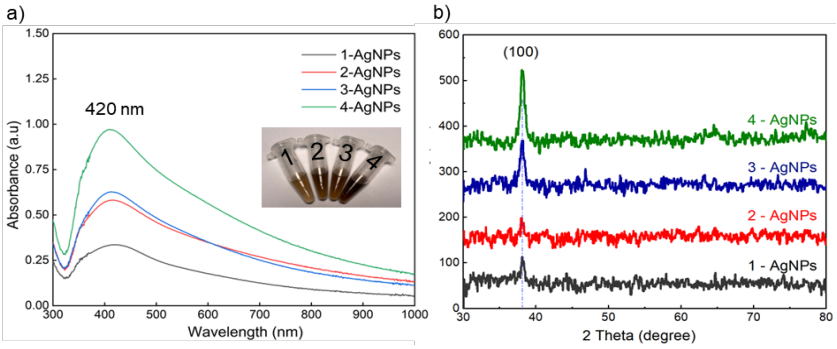


Figure 1. (a) UV-Vis absorption spectrum; (b) XRD pattern of AgNPs synthesized using *Ocimum basilicum* L. leaf extract.
Note. 1-AgNPs: treatment 1. 2-AgNPs: treatment 2. 3-AgNPs: treatment 3. 4-AgNPs: treatment 4.

The UV-Vis spectra (Figure 1a) showed a characteristic absorption peak at 410 nm corresponding to the localized surface plasmon resonance (LSPR) extinction peak of colloidal AgNPs, confirming the formation of silver nanoparticles. The absorbance intensity was directly proportional to the volume of $AgNO_3$ precursor used, reflecting the increase in the concentration of AgNPs formed. Simultaneously, no shift in the LSPR peak was observed, indicating no significant differences in the morphology and size of AgNPs among the samples. The narrow and symmetrical LSPR peak also indicates a relatively uniform distribution of AgNPs in size and shape within the solution, according to Rai et al. [2] and Vanlalveni et al. [12].

The XRD pattern, Figure 1b, shows a diffraction peak at 38.1° corresponding to the (111) crystallographic plane of metallic silver. This plane possesses the lowest surface energy and is commonly dominant in the face-centered cubic (FCC) structure of AgNPs. Because the samples were not washed by centrifugation, high concentrations of capping agents (polyphenols, flavonoids, etc.) surrounding the AgNPs produced interference signals that masked the X-ray signals from the weak lattice planes. Therefore, only the diffraction peak at the (111) plane, which has the highest intensity, was observed. The distinct peak confirms the successful reduction of silver ions to crystalline metallic silver with a crystal size of 11.81 nm calculated using the Debye-Scherrer formula. The increasing peak intensity with higher concentrations further supports the trend of increased silver phase content within the samples.

Overall, the combined UV-Vis and XRD analyses demonstrate that silver nanoparticles were successfully synthesized using basil leaf extract. The bioactive compounds in the extract likely functioned as both reducing agents and stabilizing (capping) agents for the nanoparticle surfaces. These findings provide a critical foundation for subsequent evaluation of the morphological characteristics and biological activities of the synthesized nanomaterial. The application of this "green synthesis" approach offers several significant advantages over conventional chemical methods, including cost-effectiveness, environmental sustainability, and the avoidance of toxic reagents [13, 14]. Silver nanoparticles synthesized via this method are small and uniform in particle size, which facilitates enhanced penetration through bacterial biofilms and thereby maximizes their therapeutic efficacy [15, 16].

3.2. Surface morphology and particle size distribution of AgNPs

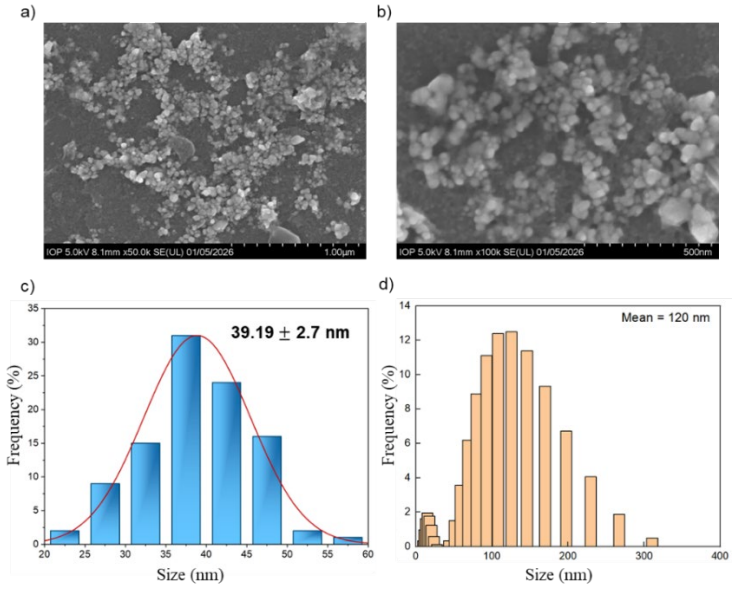


Figure 2. (a, b) SEM micrographs of AgNPs at different magnifications; (c) Particle size distribution histogram; (d) DLS spectrum of AgNPs

SEM images (Figure 2a, b) indicated that the AgNPs were predominantly quasi-spherical in shape and relatively uniformly distributed. However, slight agglomeration was observed, possibly due to incomplete coverage of the compounds in the extract across the AgNPs surfaces. At higher magnification, individual nanoparticles were clearly distinguishable, exhibiting characteristic nanoscale dimensions. The particle size distribution histogram (Figure 2c) indicated an average diameter of approximately 39.19 ± 2.7 nm, with the majority of particles distributed within the range of 30-45 nm. ImageJ software was employed to measure the size of over 100 individual nanoparticles from the SEM images. A size distribution histogram was shown in Figure 2c. The narrow size distribution and standard deviation clearly demonstrate the high monodispersity of the synthesized nanoparticles, which correlates with a low PDI value. The particle size measured from the SEM image is much larger than the crystal size at the lattice plane (111) from the XRD result, suggesting that AgNPs are polycrystalline and covered by a thick capping agent, which is consistent with the disappearance of the characteristic XRD peaks of AgNPs at the weaker lattice planes. The DLS spectrum (Figure 2d) shows the size distribution of AgNPs in solution with an average size of approximately 120 nm. This result is consistent with the slight aggregation observed in the SEM image, caused by charge imbalance and the simultaneous interaction between organic compounds and various AgNPs. This size range is considered optimal for biological activity, as smaller nanoparticles provide a larger surface area-to-volume ratio, thereby enhancing interactions with bacterial cell membranes [17]. Additionally, biologically synthesized AgNPs with sizes of 20-50 nm typically exhibit pronounced antibacterial efficacy [18]. The obtained AgNPs, with an average size of approximately 39 nm and a quasi-spherical morphology, are consistent with previous reports on biogenic silver nanoparticles. Studies by Kim et al. [19] and Sondi & Salopek-Sondi [20] indicated that smaller AgNPs (<50 nm) tend to exhibit enhanced antibacterial performance due to their increased surface area. Furthermore, comprehensive reviews by Franci et al. [21] and Shah et al. [22] emphasized the critical influence of particle size and synthesis conditions on the biological activity of AgNPs.

The stability of the nano-system was monitored via UV-Vis spectroscopy and visual observation over 3 months of storage at 4°C. As shown in Figure 3, there was no significant shift in the LSPR peak wavelength, nor was there any visible precipitation, indicating that the capping agents provide sufficient steric/electrostatic hindrance to prevent agglomeration.

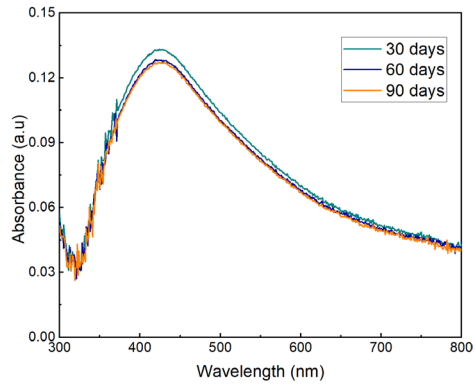


Figure 3. UV-Vis absorption spectrum of sample stored at 4°C for 90 days.

3.2. Antibacterial activity of AgNPs against E. faecalis

The selection of *E. faecalis* as the target microorganism is due to its high clinical relevance, as it is detected in approximately 30-77% of failed endodontic cases [23, 24]. This bacterium is particularly problematic due to its ability to penetrate deeply into medical devices—reaching depths of up to 1000 µm—and to form robust biofilms, which lead to significant resistance to conventional treatments [23, 25].

The antibacterial efficacy markedly increased at concentrations 3 and 4, demonstrating the dose-dependent activity of the AgNPs (Table 2).

Table 2. The effect of AgNPs synthesized from different treatments on the growth of bacteria

Treatment	Inhibition zone (mm)
Concentration 1	< 0
Concentration 2	< 0
Concentration 3	0.67 ± 0.58
Concentration 4	4.33 ± 0.58

The agar well diffusion assay demonstrated that at treatment 1 and 2, no significant inhibition zones were observed, whereas treatment 3 began to exhibit measurable antibacterial activity, and treatment 4 showed the most pronounced inhibitory effect. The negative control (NC) produced no inhibition zone, confirming that the antibacterial activity was attributable to the silver nanoparticle system.

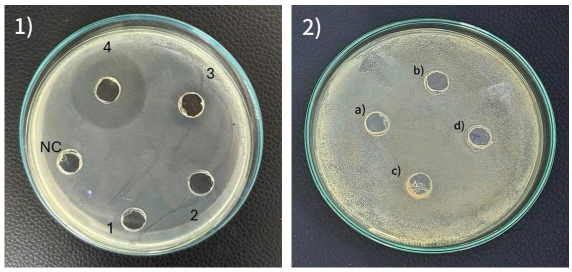


Figure 4. Agar well diffusion assay illustrating the effect of AgNPs and control groups on bacterial growth

Note: 1) Treatment from 1-4: AgNPs synthesized with silver concentrations of 0.225, 0.387, 0.419, and 0.646 nM, respectively. NC: negative control (well without any sample). 2) a,c: silver nitrate (10mM); b,d: basil extract (1/10 w/v), respectively.

From measurement, the concentration of AgNPs synthesized from each treatment from 1 to 4 were 0.225, 0.387, 0.419, and 0.646 nM, respectively. As observed in Figure 4, at the concentration of 0.419 nM, bacterial growth was inhibited. The increasing diameter of the

inhibition zones with higher concentrations indicates a clear dose-dependent antibacterial effect. This mechanism can be explained by the ability of AgNPs to adhere to the bacterial cell surface, alter membrane permeability, release Ag^+ ions, and induce intracellular oxidative stress, ultimately leading to growth inhibition and structural cell damage, as reported by Kim et al. [19] and Franci et al. [21]. Figure 4b illustrates that at the used concentration of basil extract and silver nitrate (10 mM), there were no antibacterial properties. From a phytochemical perspective, basil extracts are rich in various bioactive compounds such as phenolic acids, flavonoids, and terpenes [13, 15, 25]. These compounds play a dual role in green nanotechnology processes: they act as reducing agents facilitating the conversion of silver ions (Ag^+) into metallic silver nanoparticles (Ag^0) and simultaneously serve as natural stabilizing agents that prevent aggregation of the synthesized silver nanoparticles [13, 14].

The findings of our study are consistent with previous reports, indicating that AgNPs synthesized from basil leaf extract possess promising potential for applications in controlling infectious bacteria, particularly at higher concentrations [26].

3.3. Inhibitory effect of AgNPs on biofilm formation

Biofilms are responsible for more than 75–80% of human infections where microorganisms form highly structured and tightly adherent communities. In this state, bacteria markedly increase tolerance to antimicrobial agents greater than their planktonic cells [27]. Notably, *E. faecalis,* a pathogen found in infection, possesses the ability to form biofilms and penetrate medical devices which leads to treatment failure [23].

Since AgNPs at treatment 4 exhibited high antibacterial ability with significant difference from other treatments, it was selected to evaluate the anti-biofilm activity. Figure 5 illustrated that AgNPs at treatment 4 significantly reduced biofilm density compared to the positive control.

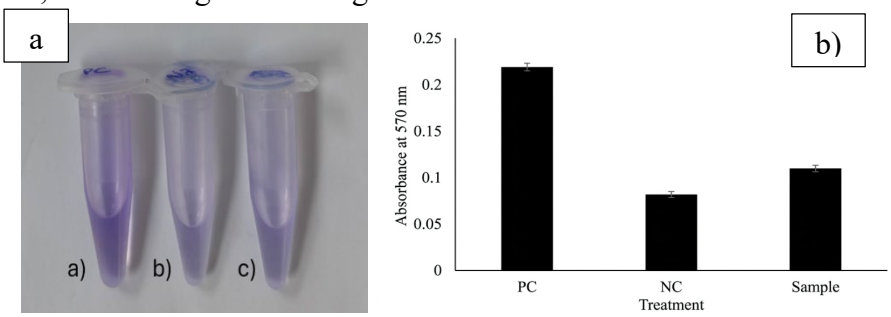


Figure 5. Anti-biofilm activity of AgNPs against *E. faecalis*. (a) Crystal violet staining of biofilms: PC (positive control: bacteria and LB medium); NC, antibiotic-treated group; Sample: AgNPs, treatment 4. (b) Quantitative analysis of biofilm biomass determined by OD570 measurement. Error bars represent standard deviation (n = 3).

The crystal violet staining assay (Figure 5a) demonstrated that the positive control exhibited the darkest purple coloration, indicating strong biofilm-forming ability. In contrast, the antibiotic-treated group and the AgNP-treated group showed substantially weaker staining intensity. Quantitative analysis of the absorbance values (Figure 5b) further confirmed that the mean optical density (OD) of the AgNP-treated group was significantly lower than that of the positive control. The AgNP-treated sample exhibited approximately 50% reduction in biofilm formation, indicating that silver nanoparticles effectively inhibited the adhesion and subsequent development of *E. faecalis* biofilms.

These findings are consistent with previous studies suggesting that AgNPs can disrupt bacterial cell membrane integrity, induce oxidative stress, and interfere with the extracellular polymeric substance (EPS) matrix, thereby inhibiting biofilm formation and stability [20, 22]. The small particle size (approximately 39 nm in this study) is a critical factor enabling silver nanoparticles (AgNPs) to penetrate the complex extracellular polymeric substance (EPS) matrix and directly interact with bacterial cells embedded within [23].

Similarly, Morones et al. [17] reported that small-sized silver nanoparticles can attach to bacterial cell surfaces, alter membrane structure, and cause leakage of intracellular components, thereby impairing biofilm formation. In addition, Lara et al. [28] demonstrated that AgNPs inhibit Gram-positive bacteria through the release of Ag^+ ions and interactions with thiol-containing proteins, leading to metabolic disruption.

Overall, the AgNPs system synthesized from plant extract exhibited not only significant antibacterial activity but also pronounced anti-biofilm efficacy, particularly at higher concentrations. These results are in agreement with recent international reports highlighting the potential application of silver nanoparticles in the management of chronic and biofilm-associated infections.

4. Conclusion

In conclusion, this study successfully synthesized AgNPs with an average size of 39.19 ± 2.7 nm using a sustainable green approach mediated by basil leaf extract (*Ocimum basilicum* L.) – a common plant in Vietnam. The synthesized nanomaterial exhibited dose-dependent antibacterial activity against *E. faecalis*. Furthermore, the anti-biofilms assay demonstrated that AgNPs effectively inhibited the formation of *E. faecalis* biofilms, resulting in a significant decrease of approximately 50% in biomass compared to the positive control. The findings prove the potential of biologically derived AgNPs as a potential and eco-friendly alternative for bacterial control, particularly in addressing persistent biofilm – associated infections. Further study should be carried out to give a deep insight into the mechanisms for anti-biofilm and antibacterial activity.

5. Funding

This research was fully funded by Tra Vinh University (TVU) under grant contract number 63/2025/HĐ.HĐKH&ĐT – ĐHTV.

References

[1] Costerton, J.W., Stewart, P.S., & Greenberg, E.P. (1999). "Bacterial biofilms: A common cause of persistent infections". *Science* (284), 1318–1322. DOI: 10.1126/science.284.5418.1318

[2] Rai, M., Yadav, A., & Gade, A. (2009). "Silver nanoparticles as a new generation of antimicrobials". *Biotechnology Advances* (27), 76–83. DOI: 10.1016/j.biotechadv.2008.09.002

[3] Durán, N., Durán, M., de Jesus, M.B., Seabra, A.B., Fávaro, W.J., & Nakazato, G. (2016). "Silver nanoparticles: A new view on mechanistic aspects of antimicrobial activity". *Nanomedicine: Nanotechnology, Biology and Medicine* (12), 789–799. DOI: 10.1016/j.nano.2015.11.016

[4] Đinh, V.H., & Nguyễn, T.P.T. (2019). "Tổng hợp nano bạc sinh học từ dịch chiết cây nha đam (*Aloe vera*) và ứng dụng kháng khuẩn". *Tạp chí Công nghệ Sinh học* (17), 55–62.

[5] Phạm, T.T.H., & Trần, T.N.M. (2020). "Nghiên cứu tổng hợp nano bạc bằng phương pháp sinh học sử dụng dịch chiết tỏi và ứng dụng lên vật liệu kháng khuẩn". *Tạp chí Khoa học và Công nghệ* (58), 101–108.

[6] Trần, T.B., & Lê, Q.D. (2021). "Tổng hợp nano bạc từ dịch chiết trà xanh và đánh giá hoạt tính kháng khuẩn đối với vi khuẩn gây bệnh thực vật". *Tạp chí Nông nghiệp và Phát triển Nông thôn* (21), 78–85.

[7] Salayová, A., Bedlovičová, Z., Daneu, N., Baláž, M., Lukáčová Bujňáková, Z., Balážová, Ľ., & Tkáčiková, Ľ. (2021). "Green synthesis of silver nanoparticles with antibacterial activity using various medicinal plant extracts: Morphology and antibacterial efficacy". *Nanomaterials* (11), 1005. DOI: 10.3390/nano11041005

[8] Haridas, E.S.H. (2025). "Bioactive silver nanoparticles derived from *Carica papaya* floral extract and its dual-functioning biomedical application". *Scientific Reports*. DOI: 10.1038/s41598-025-93864-y

[9] Abbasy, D.W.A. (2015). "Chemical composition and antibacterial activity of essential oil isolated from Omani basil (*Ocimum basilicum* Linn)". *Asian Pacific Journal of Tropical Disease*. DOI: 10.1016/S2222-1808(15)60905-7

[10] Shahrajabian, M.H. (2020). "Chemical components and pharmacological benefits of basil (*Ocimum basilicum*): A review". *International Journal of Food Properties* (23), 1961–1970. DOI: 10.1080/10942912.2020.1828456

[11] Nadeem, H.R., Akhtar, S., Sestili, P., Ismail, T., Neugart, S., Qamar, M., & Esatbeyoglu, T. (2022). "Toxicity, antioxidant activity, and phytochemicals of *Ocimum basilicum* L. leaves cultivated in Southern Punjab, Pakistan". *Foods* (11), 1239. DOI: 10.3390/foods11091239

[12] Lalveni, C., Lallianrawna, S., Biswas, A., Selvaraj, M., Changmai, B., & Rokhum, S.L. (2021). "Green synthesis of silver nanoparticles using plant extracts and their antimicrobial activities: A review of recent literature". *RSC Advances* (11), 2804–2837. DOI: 10.1039/D0RA09941D

[13] Niswah, S.U., Kusumorini, N., & Martien, R. (2026). "Development of green synthesis silver nanoparticle with *Ocimum sanctum* leaf extract: Characterization and stability study". *Majalah Farmaseutik* (22). DOI: 10.22146/farmaseutik.v22i1.113027

[14] Phạm, N.T. (2022). "Tổng hợp xanh nano bạc sử dụng dịch chiết lá chè và đánh giá hoạt tính kháng khuẩn". *Tạp chí Phân tích Hóa, Lý và Sinh học* (28).

[15] Varghese, R.M., Kumar, A., & Shanmugam, R. (2024). "Antimicrobial activity of silver nanoparticles synthesized using *Ocimum tenuiflorum* and *Ocimum gratissimum* herbal formulations". *Cureus* (16), e54994. DOI: 10.7759/cureus.54994

[16] Karakaş, İ., & Hacıoğlu Doğru, N. (2023). "Some biological potential of silver nanoparticles synthesized from *Ocimum basilicum* L.". *GSC Biological and Pharmaceutical Sciences* (22), 107–113. DOI: 10.30574/gscbps.2023.22.3.0099

[17] Morones, J.R., Elechiguerra, J.L., Camacho, A., Holt, K., Kouri, J.B., Ramírez, J.T., & Yacaman, M.J. (2005). "The bactericidal effect of silver nanoparticles". *Nanotechnology* (16), 2346–2353. DOI: 10.1088/0957-4484/16/10/059

[18] Ahmed, S., Ahmad, M., Swami, B.L., & Ikram, S. (2016). "A review on plant extract-mediated synthesis of silver nanoparticles for antimicrobial applications: A green expertise". *Journal of Advanced Research* (7), 17–28. DOI: 10.1016/j.jare.2015.02.007

[19] Kim, J.S., Kuk, E., Yu, K.N., Kim, J.-H., Park, S.J., Lee, H.J., Kim, S.H., Park, Y.K., Park, Y.H., Hwang, C.-Y., Kim, Y.-K., Lee, Y.-S., Jeong, D.H., & Cho, M.-H. (2007). "Antimicrobial effects of silver nanoparticles". *Nanomedicine: Nanotechnology, Biology and Medicine* (3), 95–101. DOI: 10.1016/j.nano.2006.12.001

[20] Sondi, I., & Salopek-Sondi, B. (2004). "Silver nanoparticles as antimicrobial agents: A case study on *E. coli* as a model for Gram-negative bacteria". *Journal of Colloid and Interface Science* (275), 177–182. DOI: 10.1016/j.jcis.2004.02.012

[21] Franci, G., Falanga, A., Galdiero, S., Palomba, L., Rai, M., Morelli, G., & Galdiero, M. (2015). "Silver nanoparticles as potential antibacterial agents". *Molecules* (20), 8856–8874. DOI: 10.3390/molecules20058856

[22] Shah, M., Fawcett, D., Sharma, S., Tripathy, S.K., & Poinern, G.E.J. (2015). "Green synthesis of metallic nanoparticles via biological entities". *Materials* (8), 7278–7308. DOI: 10.3390/ma8115377

[23] Dhara, K., Batra, D., Nagabhushan, V., Kaur, D., Chakraborty, R., & Karade, P.M. (2025). "Antibacterial activity of novel nanoparticles against persistent endodontic pathogens". *Bioinformation* (21), 4807.

[24] Trần, D.T., & Huỳnh, H.T.H. (2024). "Tính kháng khuẩn *Enterococcus faecalis* của dung dịch nano bạc và khả năng ứng dụng nano bạc trong điều trị nội nha". *Tạp chí Y học Việt Nam* (539). DOI: 10.51298/vmj.v539i2.9799

[25] Yulina, V., Herdiyati, Y., & Chemiawan, E. (2024). "In vitro antibiofilm evaluation of *Ocimum basilicum* extracts against *Enterococcus faecalis*". *Majalah Kedokteran Gigi* (10), 38. DOI: 10.22146/majkedgiind.84185

[26] Trịnh, T.H., Vũ, T.N., Nguyễn, N.M.T., Lai, T.Q., & Trần, D. (2025). "Đặc điểm kháng kháng sinh của *Enterococcus faecalis* và *Enterococcus faecium* tại Bệnh viện Hữu nghị Việt Tiệp Hải Phòng năm 2024". *Tạp chí Khoa học Sức khỏe* (3). DOI: 10.59070/jhs030125004

[27] Ottoni, C.A., Simões, M.F., Fernandes, S., dos Santos, J.G., da Silva, E.S., de Souza, R.F., et al. (2016). "Screening of filamentous fungi for antimicrobial silver nanoparticles synthesis". *Frontiers in Microbiology* (7), 592. DOI: 10.3389/fmicb.2016.00592

[28] Lara, H.H., Ayala-Nuñez, N.V., Ixtepan-Turrent, L., & Rodriguez-Padilla, C. (2010). "Mode of antiviral action of silver nanoparticles against HIV-1". *Journal of Nanobiotechnology* (8), 1. DOI: 10.1186/1477-3155-8-1.